The Dynamic Beamformer

Ali Bahramisharif[1,2], Marcel A.J. van Gerven[2,1], Jan-Mathijs Schoffelen[2], Zoubin Ghahramani[3], and Tom Heskes[1,2]

[1] Radboud University Nijmegen, Institute for Computing and Information Sciences, Nijmegen, The Netherlands
[2] Radboud University Nijmegen, Donders Institute for Brain, Cognition and Behaviour, Nijmegen, The Netherlands
[3] Department of Engineering, University of Cambridge, Cambridge, UK

1 Introduction

As the number of possible neural sources is much higher than the number of MEG or EEG sensor readings, the inverse problem of estimating source amplitudes from sensor readings has many solutions. A common approach to tackle this problem is to assume that all sources are independent from each other.This approach is widely used in the neuroscience community and is known as beamforming [6, 8, 5, 7].

Since the source amplitude is likely to change smoothly over time, we expect to improve the source localization by taking the temporal dynamics into account. Smoothness constraints have been combined with source localization in a Bayesian framework [13, 9, 16]. Specifically, the Kalman filter and particle filter have been introduced in the context of EEG and MEG source localization based on dipole-fitting approaches [1, 2]. The model introduced in [1, 2] relies on the integration of many dynamic dipolar neural models. In this paper, in contrast to the dipole-fitting approach, we incorporate the independence assumption of the standard beamformer in a linear dynamic system, and we show that by using the leadfield matrix as the observation model and setting the covariance of the observation noise to be proportional to the covariance of the observation, we arrive at the dynamic beamformer.

2 Method

2.1 Beamforming

Let m, n, and T denote the number of sources, sensors, and samples, respectively. The goal of source localization is to estimate active sources $S \in \mathbb{R}^{m \times T}$ from sensor readings $X \in \mathbb{R}^{n \times T}$. In the source localization problem, sources are assumed to project linearly to the sensors via a leadfield matrix $L \in \mathbb{R}^{n \times m}$.

* AB, MG, JS, and TH gratefully acknowledge the support of the BrainGain Smart Mix Programme of the Netherlands Ministry of Economic Affairs and the Netherlands Ministry of Education, Culture and Science.

In other words, $X = LS$, where L and X are given and S is to be estimated. If we further assume that the solution to the source localization problem can be written as a linear mapping from sensors to sources, the problem of source localization reduces to estimating the linear projection matrix $W \in \mathbb{R}^{n \times m}$ that projects the sensors to the sources; in other words: $S = W'X$.

Beamforming derives from the assumption that the sources are uncorrelated. Defining $\mathbf{s}_i \equiv S_{i\cdot}, \boldsymbol{\ell}_i \equiv L_{\cdot i}$, and $\mathbf{w}_i \equiv W_{\cdot i}$, for each source $\mathbf{s}_i \equiv (\mathrm{s}_{i,1}, \ldots, \mathrm{s}_{i,T})$, we can write: $\mathbf{s}_i = \mathbf{w}_i' X = \mathbf{w}_i' \boldsymbol{\ell}_i \mathbf{s}_i$, which implies that $\mathbf{w}_i' \boldsymbol{\ell}_i = 1$ for all $i \in 1, \ldots, m$. A standard approach is to minimize the variance of the sources and find the $\mathbf{w}_i$ which minimizes $\mathbf{s}_i \mathbf{s}_i' = \mathbf{w}_i' \Sigma \mathbf{w}_i$ subject to $\mathbf{w}_i' \boldsymbol{\ell}_i = 1$, where $\Sigma \equiv XX'$. The solution is shown to be [15]:

$$\mathbf{s}_i = (\boldsymbol{\ell}_i' \Sigma^{-1} \boldsymbol{\ell}_i)^{-1} \boldsymbol{\ell}_i' \Sigma^{-1} X \tag{1}$$

for all $i \in 1, \ldots, m$.

2.2 Generalized least squares problem

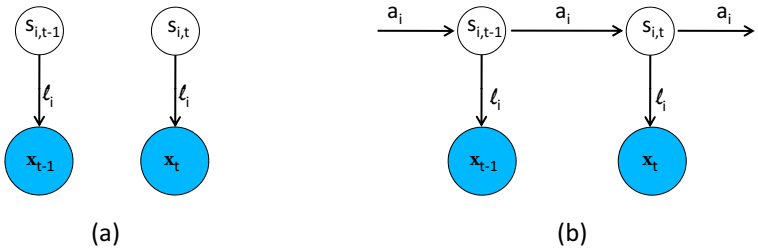

Fig. 1. (a) Graphical representation of a linear Gaussian model. (b) Graphical representation of the dynamic beamformer.

The beamformer can be interpreted as a specific kind of linear probabilistic model. Assume that we have a linear Gaussian model, as shown in Fig. 1a, in which $\mathbf{x}_t \equiv X_{\cdot t}$ is the observation at time t where $1 \leq t \leq T$, and $\boldsymbol{\ell}_i$ is given. We can write the equation for the model as $\mathbf{x}_t = \boldsymbol{\ell}_i \mathrm{s}_{i,t} + \mathbf{u}_{i,t}$, where $\mathbf{u}_{i,t} \sim \mathcal{N}(0, R)$. Now we try to find $\mathbf{s}_i$ which maximizes the likelihood of the parameters given the observations and R. Ignoring the constant terms, the negative log-likelihood can be written as $\frac{1}{2}(X - \boldsymbol{\ell}_i \mathbf{s}_i)' R^{-1} (X - \boldsymbol{\ell}_i \mathbf{s}_i)$, which is minimized by taking:

$$\mathbf{s}_i = \left(\boldsymbol{\ell}_i' R^{-1} \boldsymbol{\ell}_i\right)^{-1} \boldsymbol{\ell}_i' R^{-1} X \,. \tag{2}$$

Comparing Eqs. 1 and 2, we see that setting R proportional to Σ, it is evident that the model depicted in Fig. 1a is equivalent to the standard beamformer. In other words, a linear Gaussian model is a beamformer, if we assume that the covariance of the observation noise is proportional to the covariance of the observations and use the leadfield matrix as the observation model.

2.3 Dynamic beamforming

The correspondence between the beamformer and the linear Gaussian model suggests that the same correspondence holds for the linear dynamic system. We propose that the dynamic beamformer can be obtained by just using the leadfield matrix as the observation model of a linear dynamic system and setting the covariance of the observation noise to be proportional to the covariance of the observation. The graphical model of the dynamic beamformer is shown in Fig. 1b. For each source $\mathbf{s}_i \equiv (\mathrm{s}_{i,1}, \ldots, \mathrm{s}_{i,T})$, dynamic beamforming can be mathematically expressed as:

$$\mathbf{x}_t = \boldsymbol{\ell}_i \mathrm{s}_{i,t} + \mathbf{u}_{i,t} \tag{3}$$

$$\mathrm{s}_{i,t} = \mathrm{a}_i \mathrm{s}_{i,t-1} + v_{i,t} \tag{4}$$

where $\mathbf{u}_{i,t} \sim\mathcal{N}(0, \alpha_i \Sigma)$ and $v_{i,t} \sim\mathcal{N}(0, q_i)$ independently for $i \in 1, \ldots, m$ and $1 \leq t \leq T$. Note that $\mathrm{s}_{i,t}$ and so a_i and q_i are scalar values. Note further that each $\mathbf{s}_i$ should be predictive for the full observation X, so there is no i in the left hand side of Eq. 3. Following the equations reported in [14], we can find a_i, q_i, α_i, and $\mathbf{s}_i$ by means of an expectation maximization algorithm.

3 Results and discussion

We evaluated our method using data of the best performing subject reported in [3]. The subject's task was to maintain central fixation while covertly attending to a target which followed a circular trajectory. The condition was given by the sine and cosine of the angles between the target and the positive x-axis over time. To construct the leadfield matrix, we used a structural MRI and the head model developed in [10]. Then we discretized the brain volume into a grid with $1 \times 1 \times 1\,\mathrm{cm}^3$ resolution. For each grid point the leadfield was calculated. Preprocessing and leadfield generation was done using FieldTrip [11].

The complexity of the dynamic beamformer increases with the number of time points. As shown in [3] that task-specific information for this data shows up as modulations of occipital alpha power (8-12 Hz) in the frequency domain, applying the dynamic beamformer on the frequency domain results in a much lower process time. In this study we used a linear trick for power extraction in order not to violate the linearity of the beamformer. Imagine that we have a reference signal which has the same frequency and the same phase as the signal that we want to decode. We take the Fourier transform of the data, which is a linear operation, only focusing on the desired frequency, and subtract the phase of the reference signal. Then, the real part of the Fourier transform would represent the amplitude of the signal which, averaged over a time window, results in an estimate of the power of the signal over that frequency [12].

We computed the absolute correlation of the sources reconstructed using both the beamformer and the dynamic beamformer with the experimental design which, in our case, is given by the sine and cosine of the direction of attention. As shown in Fig. 2a, occipital sources are more correlated with the

experimental design in the dynamic beamformer reconstruction. These occipital sources are known to be involved when subjects are covertly attending to a peripheral target [4]. Here, the higher correlation is expected, as the experimental design changes very smoothly and the dynamic beamformer enforces the smooth transition of the sources which can result in a higher correlation.

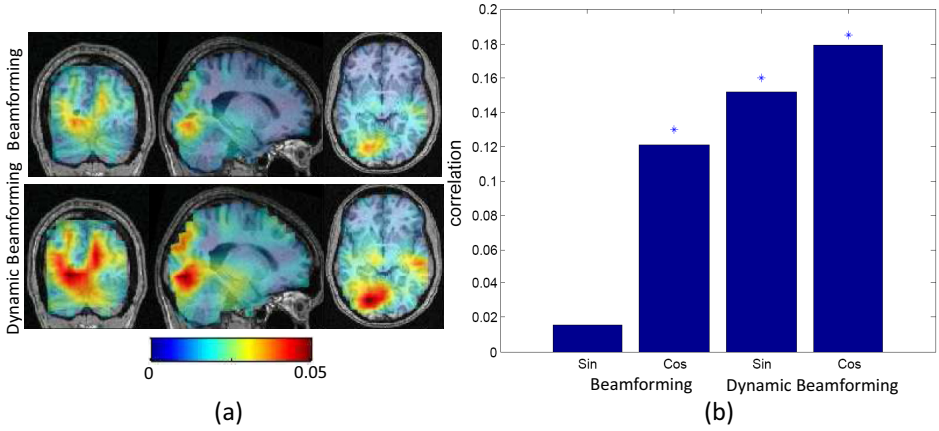

Fig. 2. (a) Correlation of the sources reconstructed using both the beamformer and the dynamic beamformer with the experimental conditions. (b) Correlation of the predicted experimental design based on the sources reconstructed using either the beamformer or the dynamic beamformer. Significant correlations ($p < 0.001$) are marked with a '*'.

We validated our method by decoding the experimental design from the source estimates. We used 25 minutes of data for training two L2 regularized linear regressors to predict sine and cosine of the direction of attention and 5 minutes for testing them. Figure 2b shows the correlation of the predictions for sine and cosine based on the sources reconstructed using the beamformer and the dynamic beamformer with the true values. As shown, the dynamic beamformer results in a better prediction of the conditions than the standard beamformer. Specifically, the dynamic beamformer is performing much better for the sine component of the angle than the standard version. As the sign of the cosine and sine represent left versus right and up versus down, respectively, Fig. 2b implies that it is more difficult to discriminate up from down than left from right using the sources reconstructed with standard beamforming.

Our validation shows that the dynamic beamformer outperforms the standard beamformer in predicting the conditions, which strongly suggests that it also outperforms the standard approach in estimating the active neural generators.

References

1. J.M. Antelis and J. Minguez. Dynamic solution to the EEG source localization problem using Kalman filters and particle filters. In *Annual International Conference of the IEEE Engineering in Medicine and Biology Society (EMBC)*, pages 77–80, 2009.
2. J.M. Antelis and J. Minguez. DYNAMO: Dynamic multi-model source localization method for EEG and/or MEG. In *Annual International Conference of the IEEE Engineering in Medicine and Biology Society (EMBC)*, pages 5141–5144, 2010.
3. A. Bahramisharif, M.A.J. van Gerven, T. Heskes, and O. Jensen. Covert attention allows for continuous control of brain-computer interfaces. *Eur. J. Neurosci.*, 31(8):1501–1508, 2010.
4. M.S. Beauchamp, L. Petit, T.M. Ellmore, J. Ingeholm, and J.V. Haxby. A parametric fMRI study of overt and covert shifts of visuospatial attention. *NeuroImage*, 14(2):310–321, 2001.
5. A.M. Dale, A.K. Liu, B.R. Fischl, R.L. Buckner, J.W. Belliveau, J.D. Lewine, and E. Halgren. Dynamic statistical parametric mapping: Combining fMRI and MEG for high-resolution imaging of cortical activity. *Neuron*, 26(1):55–67, 2000.
6. A.M. Dale and M.I. Sereno. Improved localizadon of cortical activity by combining EEG and MEG with MRI cortical surface reconstruction: a linear approach. *J. Cognitive Neurosci.*, 5(2):162–176, 1993.
7. J. Gross, J. Kujala, M. Hämäläinen, L. Timmermann, A. Schnitzler, and R. Salmelin. Dynamic imaging of coherent sources: studying neural interactions in the human brain. *P. Natl. Acad. Sci. USA*, 98(2):694–699, 2001.
8. M.S. Hämäläinen and R.J. Ilmoniemi. Interpreting magnetic fields of the brain: minimum norm estimates. *Med. Biol. Eng. Comput.*, 32(1):35–42, 1994.
9. J. Mattout, C. Phillips, W.D. Penny, M.D. Rugg, and K.J. Friston. MEG source localization under multiple constraints: an extended Bayesian framework. *NeuroImage*, 30(3):753–767, 2006.
10. G. Nolte. The magnetic lead field theorem in the quasi-static approximation and its use for magnetoencephalography forward calculation in realistic volume conductors. *Phys. Med. Biol.*, 48:3637–3652, 2003.
11. R. Oostenveld, P. Fries, E. Maris, and J.M. Schoffelen. FieldTrip: open source software for advanced analysis of MEG, EEG, and invasive electrophysiological data. *Computat. Intell. Neurosc.*, 2011:1, 2011.
12. A.V. Oppenheim, A.S. Willsky, and S.H. Nawab. *Signals and systems*. Pearson education, 1998.
13. W. Penny, S. Kiebel, and K. Friston. Variational Bayesian inference for fMRI time series. *NeuroImage*, 19(3):727–741, 2003.
14. S. Roweis and Z. Ghahramani. A unifying review of linear Gaussian models. *Neural Comput.*, 11(2):305–345, 1999.
15. B.D. Van Veen, W. van Drongelen, M. Yuchtman, and A. Suzuki. Localization of brain electrical activity via linearly constrained minimum variance spatial filtering. *IEEE T. Bio-Med. Eng.*, 44(9):867–880, 1997.
16. D. Wipf and S. Nagarajan. A unified Bayesian framework for MEG/EEG source imaging. *NeuroImage*, 44(3):947–966, 2009.